Title
Evolution of Grain Structure during Disorder-to-Order Transitions in a Block Copolymer/Salt Mixture Studied by Depolarized Light Scattering

Journal
Macromolecules, 47(16)

ISSN
0024-9297

Authors
Wang, Xin
Thelen, Jacob L
Teran, Alexander A
et al.

Publication Date
2014-08-26

DOI
10.1021/ma501166p

Peer reviewed

Macromolecules

Article

pubs.acs.org/Macromolecules

Evolution of Grain Structure during Disorder-to-Order Transitions in a Block Copolymer/Salt Mixture Studied by Depolarized Light Scattering

Xin Wang,[†] Jacob L. Thelen,[‡,§] Alexander A. Teran,[‡,§] Mahati Chintapalli,[∥,§] Issei Nakamura,[⊥,¶] Zhen-Gang Wang,[⊥] Maurice C. Newstein,[#] Nitash P. Balsara,[‡,§,○] and Bruce A. Garetz[†,*]

[†]Department of Chemical and Biomolecular Engineering, NYU Polytechnic School of Engineering, Brooklyn, New York 11201, United States

[‡]Department of Chemical and Biomolecular Engineering, University of California, Berkeley, California 94720, United States

[§]Environmental Energy Technologies Division, Lawrence Berkeley National Laboratory, Berkeley, California 94720, United States

[∥]Department of Materials Science and Engineering, University of California, Berkeley, California 94720, United States

[⊥]Division of Chemistry and Chemical Engineering, California Institute of Technology, Pasadena, California 91125, United States

[#]Department of Electrical and Computer Engineering, NYU Polytechnic School of Engineering, Brooklyn, New York 11201, United States

[○]Materials Sciences Division, Lawrence Berkeley National Laboratory, Berkeley, California 94720, United States

ABSTRACT: Block copolymer/lithium salt mixtures are promising materials for lithium battery electrolytes. The growth of ordered lamellar grains after a block copolymer electrolyte was quenched from the disordered state to the ordered state was studied by depolarized light scattering. Three quench depths below the order-to-disorder transition temperature were studied: 6, 12, and 24 °C. Regardless of quench depth, elongated ellipsoidal grains with aspect ratios between six and eight were formed during the initial stage of order formation. This was followed by a rapid reduction in aspect ratio; at long times, isotropic grains with aspect ratios in the vicinity of unity were obtained. Unusual grain growth kinetics were observed at all quench depths: (1) The average grain volume decreased with time after the early stage of grain growth. To our knowledge, a decrease in grain size has never been observed before in any quenched block copolymer system. (2) The volume fraction occupied by ordered grains of the shallowest quenched sample (quench depth of 6 °C) was significantly less than unity even after waiting times approaching 400 min. This is consistent with recent theoretical and experimental work indicating the presence of a coexistence window between ordered and disordered phases due to the partitioning of the salt into the ordered domains. At quench depths of 12 and 24 °C, which are outside the coexistence window, the grain volume fraction increases monotonically with time, and ordered grains occupy the entire sample at long times.

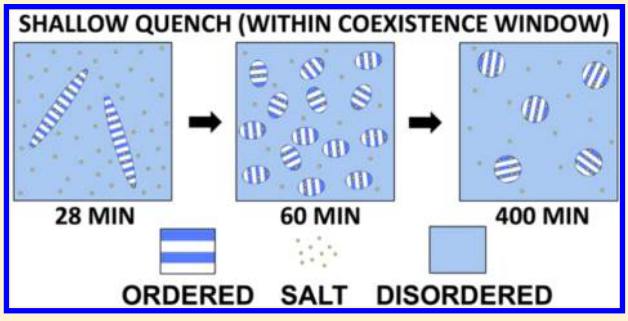

INTRODUCTION

Nanostructured mixtures of salts and block copolymers are promising solid electrolytes for rechargeable batteries with lithium metal anodes.[1−3] It has been demonstrated that electrolytes with lamellar morphologies comprising alternating soft conducting domains and rigid insulating domains resist lithium dendrite growth, increasing the lifespan of the battery.[4]

The thermodynamics[5−9] and kinetics[10−13] of order formation in A-B diblock copolymers are well established. These systems exhibit a sharp, first-order, order-to-disorder transition (ODT). When disordered samples are cooled below the order-to-disorder transition temperature, T_{ODT}, the ordered phase begins to grow. Coherent order is restricted to micron-sized regions that are often referred to as grains. During the early stage, grains grow rapidly at the expense of the disordered phase until ordered grains occupy the entire sample. This is followed by a slow growth phase where grain size increases due to defect annihilation. In some cases, defect annihilation is so slow that no change in average grain volume can be detected experimentally. Our understanding of the evolution of grain structure in block copolymers is based on time-resolved depolarized light scattering,[5,10−12,14] microscopy,[15−24] and other techniques.[25]

In contrast, neither the thermodynamics nor the kinetics of order formation in mixtures of salts and A−B diblock copolymers is well established. One of the blocks must be polar to selectively dissolve the salt. Early work suggested that the thermodynamics of these systems was similar to that of

Received: June 4, 2014
Revised: July 30, 2014
Published: August 12, 2014

   dx.doi.org/10.1021/ma501166p | Macromolecules 2014, 47, 5784−5792

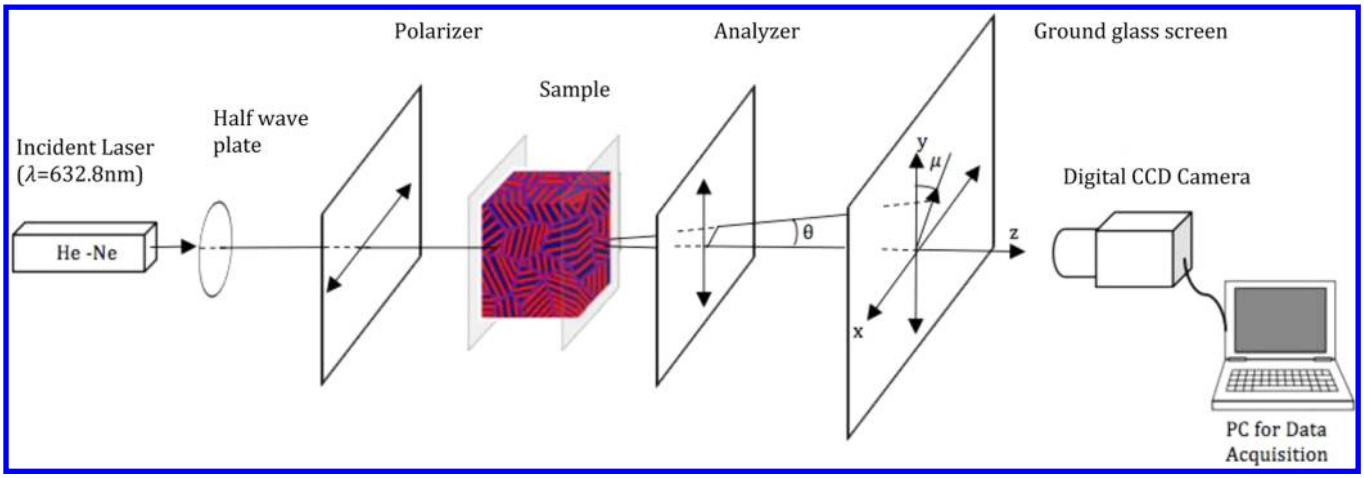

Figure 1. Schematic of depolarized light scattering apparatus and scattering geometry. A scattered light ray deflected from the forward direction is characterized by the angles θ and μ.

pure block copolymers provided the effective Flory–Huggins interaction parameter between the blocks, χ, was recast to account for the increased "effective" repulsion between the salt-containing polar block and the salt-free nonpolar block.[26−34] However, the addition of salt—another component—to a neat A–B diblock copolymer melt makes the resulting system a binary mixture. According to the Gibbs phase rule, phase coexistence is generally expected for all the order–disorder and order–order transitions. Recent theoretical and experimental work indicates the phase behavior of salt-containing block copolymers is fundamentally different from that of neat block copolymers.[26,28,29,35−37] Thelen et al.[37] used small-angle X-ray scattering (SAXS) to show that a mixture of polystyrene-*b*-poly(ethylene oxide) (SEO) with lithium bis(trifluoromethanesulfonyl)imide (LiTFSI) exhibits an ODT that extends over an 11 °C window, in which there is coexistence of ordered and disordered phases. The observed coexistence region is consistent with that predicted by Nakamura et al.[36] who suggested that this phenomenon is due to the selective partitioning of salt into the ordered phase. Because of the selective partitioning of the salt in the two coexisting phases, the evolution of order as the system is quenched from the disordered phase to the coexistence region is accompanied by a redistribution of salt ions between the two phases.

In this paper, we present the first study of the kinetics of grain growth in a salt/block copolymer mixture, quenched from the disordered state to the ordered state, using depolarized light scattering (DPLS). In order to facilitate our understanding of the relationship between thermodynamics and kinetics, we use the same SEO/LiTFSI mixture as that used by Thelen et al.[37] We show that for shallow quenches, the kinetics of grain growth in these systems is very different from that seen in neat block copolymers. In particular, at the shallowest quench depth, the average grain size first increases with time and then decreases, and the volume fraction of the sample occupied by ordered grains is less than unity at long times. In contrast, the kinetics at large quench depths is similar to that of neat block copolymers; the volume fraction of the sample occupied by ordered grains is in the vicinity of unity at long times.

EXPERIMENTAL SECTION

Materials. In this study, the polystyrene-*b*-poly(ethylene oxide) (SEO) diblock copolymers were synthesized, purified, characterized and finally doped with lithium bis(trifluoromethanesulfonyl)imide (LiTFSI) as described in ref 37. The electrolyte mixture used in this study was prepared by mixing SEO(1.7−1.4) and LiTFSI to obtain a salt concentration of r = 0.075, where r is the ratio of Li^+ ions to ethylene oxide monomer units. The block copolymers used in this study are abbreviated as SEO(xx–yy), where xx and yy are the values of M_{PS} and M_{PEO}, the number-averaged molecular weights of the polystyrene (PS) and poly(ethylene oxide) (PEO) blocks in kg mol^{-1}, respectively.

The light scattering samples were prepared by melt-forming the dried electrolyte mixture (SEO/LiTFSI) into a 1/32-in thick Viton spacer with an inner diameter of 3/16 in on a quartz disk placed on a hot plate set to 100 °C. A second quartz disk was then placed on top to sandwich the electrolyte. The electrolyte samples thus obtained were transparent with no bubbles. The samples were then placed in custom-designed air-free aluminum sample holders with an open window in the center allowing the transmission of a laser beam and scattered light. The thickness of the sample material was approximately 0.8 mm. The sample was then sealed in a pouch in an argon glovebox. The steps described above were conducted at Berkeley. The pouched samples were shipped to Brooklyn for the light scattering studies.

DPLS and Birefringence Measurements.[38] The depolarized light scattering measurements were performed on a custom-made apparatus following the principles described in ref 38. A schematic of the apparatus is shown in Figure 1. The light source was a continuous-wave helium–neon laser with a wavelength of 633 nm and an output power of 15 mW. A half-wave plate, placed between the laser and the first polarizer, could be rotated to control the light intensity incident on the sample. The sample holder was placed in an aluminum heating block insulated with a fiberglass jacket. The heating block was electrically heated by two heating elements within the block and cooled by ambient air. The sample temperature was controlled using an Omega Engineering temperature controller (CN9111A). To determine the relationship between the temperature measured by the controller and the actual sample temperature, a separate experiment was conducted, monitoring the edge temperature of the sample holders and the temperature at the center of the sample in the holders. The edge temperature was measured directly by the controller, while the temperature at center of the sample was measured by inserting an insulated thin wire thermocouple into the sample material in a used sample holder.

After transmission through the sample, the scattered laser light passed through the analyzer whose transmission axis was rotated 90 deg relative to the transmission axis of the polarizer. A Lumenera CCD camera (INFINITY2-1R) was used to record the scattering patterns incident on an Edmundoptics ground glass screen.

The birefringence method[39] was used determine the order–disorder transition temperatures of the light scattering samples,

dx.doi.org/10.1021/ma501166p | Macromolecules 2014, 47, 5784−5792

T_{ODT}. In this method, the total depolarized transmitted laser power was monitored as the sample was heated. When the sample is heated above the T_{ODT}, it becomes completely disordered, and the total transmitted power goes to zero. For the three samples studied in this paper, the minimum temperature required for complete extinction of the total transmitted light power was 124 ± 2 °C, which we took to be the T_{ODT} of the system.

At the beginning of the depolarized light scattering experiments, the laser was warmed up for 2 h to ensure a constant laser power. The sample was then placed into the heating block and initially heated to 140 °C (16 °C above T_{ODT}) for 30 min to disorder the sample and to erase any thermal and processing history. At this point, the SEO/LiTFSI mixture was in a fully disordered state, and no light was transmitted through the cross polarizers. To locate the center of the scattering pattern on the screen, the analyzer was slightly uncrossed temporarily with respect to the polarizer, allowing a small portion of incident laser beam to leak through to the screen, where it formed a small spot, whose coordinates were recorded as the center of scattering pattern. After the disordering period, the quenching process began when the temperature controller was set to the target quench temperature, and at the same time, the data acquisition system was activated to begin recording the scattering patterns. Samples were quenched to the final quench temperatures of 118, 112, and 100 °C, which will be referred to in terms of the corresponding quench depths (6, 12, and 24 °C, respectively) in the following sections of this paper. The times taken to reach the final quench temperatures of 118, 112, and 100 °C were 6, 12, and 35 min, respectively. These time periods were determined in separate experiments using a thin wire thermocouple placed in a used sample holder and connected to an Omega HH306A automated thermometer. The thermal conditions used to record the time dependence of the sample temperature during quenches were identical to those used in the depolarized light scattering experiments.

The first pattern was captured at the moment the temperature controller was set to the final quench temperature, and this time point was defined to be 0 min, the start of the quenching process. The first pattern was treated as a background noise pattern that was subtracted from subsequent patterns. The last pattern was captured 400 min after the start of the quenching process; this constituted the end of the quench. Scattering patterns were recorded every minute in the first hour, and then every 10 min until the end of the quench. The scattering patterns were stored in the form of 480 × 640 pixel TIFF image files.

DPLS Data Reduction and Analysis. During the quenching process, ordered, randomly oriented, lamellar regions are formed that exhibit form birefringence, with an optic axis that is perpendicular to the local lamellar planes. For simplicity, we consider a random collection of birefringent grains in which the optic axis has a constant orientation. The grains are assumed to be ellipsoids of revolution on average, with an optic axis parallel to the shape axis; they are characterized by their average length and width, l and w, and they have an isotropic orientation distribution. We have used this model to characterize several block copolymer melts and solutions in previous studies.[5,10,11,14,40] In the past, theoretical scattering patterns were computed by numerical integration of the governing equations. In this paper, we present analytical expressions for the scattering profiles.

The intensity of the scattered light illuminating the ground glass screen can be described as $I(x,y)$, where x and y are the Cartesian coordinates of a point on the screen relative to an origin at the center of the scattering pattern. From the coordinates (x,y) one can calculate polar and azimuthal scattering angles μ and θ according to

$$\mu = \tan^{-1}\left(\frac{y}{x}\right) \tag{1}$$

$$\theta = \tan^{-1}\left(\frac{\sqrt{x^2 + y^2}}{d}\right) \tag{2}$$

where d is the distance between the sample and the screen, which is 40.2 cm in these experiments. From θ, one can calculate magnitude of the scattering vector $q = 4\pi\lambda^{-1}\sin(\theta/2)$, where λ is the wavelength of the light. The scattered intensity can thus be described as a function of q and μ. We have shown previously[11] that for uncorrelated ellipsoidal grains, the scattered intensity can be expressed as the sum of two terms, one that is independent of μ and the other that is 4-fold symmetric in μ:

$$I(q, \mu) = I_0[C_0(q; l, w) + C_4(q; l, w)\cos 4\mu] \tag{3}$$

where I_0 is the intensity in the forward direction. The physical origins of the 4-fold spatial symmetry are discussed in ref 11, and it arises from correlations between the axis that defines the shape of the grains and the optic axis of the grain. The simplest grain structure consistent with this scattering pattern is a collection of randomly oriented ellipsoidal grains with optic axes coincident with the axis of rotation of the ellipsoid. The $C_0(q;l,w)$ component dictates the overall decay of the scattered intensity as a function of q, l and w; the $C_4(q;l,w)$ component is a measure of the depth of the 4-fold modulation of the scattering patterns. $C_0(q;l,w)$ and $C_4(q;l,w)$ are normalized such that $C_0(0;l,w) = 1$ and $C_4(0;l,w) = 0$. The equations in ref 11 were integrated using *Mathematica* to yield analytical expressions for $C_0(q;l,w)$ and $C_4(q;l,w)$ within the single ellipsoidal grain model:

$$C_0(q; l, w) = \frac{15}{4096\alpha^{5/2}}\exp\left[-\left(\frac{qw}{2}\right)^2\right]\{-4e^{-2\alpha}\alpha^{1/2}(9 + 20\alpha) + (2\pi)^{1/2}[9 + 8\alpha(1 + 6\alpha)]\,\mathrm{erf}[(2\alpha)^{1/2}]\} \tag{4}$$

$$C_4(q; l, w) = \frac{15}{4096\alpha^{5/2}}\exp\left[-\left(\frac{qw}{2}\right)^2\right]\{-20e^{-2\alpha}\alpha^{1/2}(21 + 4\alpha) + 3(2\pi)^{1/2}[35 + 8\alpha(-5 + 2\alpha)]\,\mathrm{erf}[(2\alpha)^{1/2}]\} \tag{5}$$

where

$$\alpha = \frac{(qw)^2}{8}\left(\left(\frac{l}{w}\right)^2 - 1\right) \tag{6}$$

In our analysis of an experimental scattering pattern, we can extract the two cosine moments $f_0(q)$ and $f_4(q)$ using the equations:

$$f_0(q) = \int_0^{2\pi} I(q, \mu)\,\mathrm{d}\mu = 2\pi I_0 C_0(q; l, w) \tag{7}$$

$$f_4(q) = \int_0^{2\pi} I(q, \mu)\cos 4\mu\,\mathrm{d}\mu = \pi I_0 C_4(q; l, w) \tag{8}$$

The experimental $I(q,\mu)$ data were numerically integrated to yield $f_0(q)$ and $f_4(q)$. By least-squares fitting of the experimentally extracted functions $f_0(q)$ and $f_4(q)$ to $2\pi I_0 C_0(q;l,w)$ and $\pi I_0 C_4(q;l,w)$(see eqs 4−6), respectively, we obtained estimates of l, w and I_0. In the fitting, the relative weights of $f_0(q)$ and $f_4(q)$ were taken to be 0.99 and 0.01, respectively. We cannot use scattering data collected near $q = 0$ to obtain I_0 in our analysis because of leakage of the incident laser beam at small scattering angles.

When a sample consists of a mixture of ordered and disordered regions, the volume fraction occupied by grains, ϕ, can be calculated from the following equation,[11]

$$I_0 = K\phi V \tag{9}$$

where V is the average grain volume ($V = l \times w^2$), and K is a proportionality constant that depends on the geometrical configuration of the experiment, on n, the average refractive index of the sample, and on Δn^2, the square of the form birefringence of the grains. Both n and Δn^2 are functions of temperature and wavelength.

The birefringence signal is the ratio of the total depolarized scattered power, P, to the incident laser power, P_0, which for the simple ellipsoidal grain model, is given by

dx.doi.org/10.1021/ma501166p | Macromolecules 2014, 47, 5784−5792

$$P/P_0 = \frac{\pi^{5/2}}{4}\phi\Delta n^2\frac{L_S w}{\lambda^2}f(a) \tag{10}$$

$$f(a) = \frac{1}{4a^4}\left[\sqrt{1-a^2}(6a^2-3) + (3-8a^2+8a^4)\frac{\arcsin a}{a}\right] \tag{11}$$

$$a = \sqrt{1-(w/l)^2} \tag{12}$$

where L_S is the sample thickness. This signal is thus proportional to ϕ and Δn^2. For a completely disordered sample, P/P_0 =0.

Typical results of birefringence experiments near the T_{ODT} are shown in Figure 2 where the signal, P/P_0, is plotted as a function of time for a series of step changes in sample temperature. The sample was first disordered and then quenched to 25 ± 1 °C. It is reasonable to assume that the sample was filled with ordered grains at 25 °C; i.e., ϕ = 1. P/P_0 is insensitive to changes in temperature in the 25−110 °C window. The step change in temperature from 85 to 110 °C shown at times from 0 to 30 min, has no effect on P/P_0 suggesting that Δn_2, ϕ and V are unaffected by this step (eq 10). In contrast, a step change in temperature from 110 to 112 °C results in a decrease in P/P_0, but with an unstable increasing value. We do not expect a large change in Δn^2 for such a small temperature change. We thus conclude that changes in P/P_0 reflect changes in ϕ and V.[25] We anticipate the possibility of a coexistence window; thus, the decrease in P/P_0 is probably due to a decrease in ϕ. We are not sure of the origin of the nonmonotonic time dependence of P/P_0 during this step. It is possible that the average grain size increases when the sample is annealed in the coexistence window. The step change from 112 to 120 °C leads to a further decrease in P/P_0 to a stable nonzero value. This indicates that 120 °C is also within the coexistence window. The birefringence signal is zero at temperatures ≥124 °C, indicating that the sample is disordered in this range. These experiments indicate that order−disorder coexistence occurs in this sample in the 112−124 °C window. We examined 3 different samples, and the range for the lower limit of the coexistence window was 112−118 °C while the range for the upper limit of the coexistence window was 122−126 °C. This is qualitatively consistent with the data presented in ref 37; although the transition temperatures vary by as much as 20 °C, the width of the coexistence regions is the same within experimental error. We attribute this discrepancy to the extreme sensitivity of the thermodynamics of salt/block copolymer mixtures to small changes in salt concentration (and perhaps the presence of small amounts of contaminants like water).[28] We define the lower bound of the order−disorder coexistence window as T_{OCT}, namely, the order-to-coexistence transition temperature, while the upper bound is the same as the T_{ODT} (order-to-disorder transition temperature). Below T_{OCT}, the sample remains in the fully ordered state (see Figure 2), and above the T_{ODT}, the sample is completely disordered by heating; the coexistence of ordered and disordered phases occurs at temperatures between T_{OCT} and T_{ODT}.

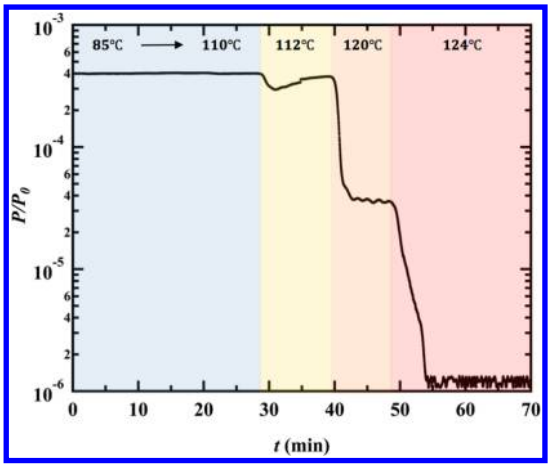

Figure 2. Plot of birefringence signal P/P_0 as an ordered sample was heated from room temperature up to the T_{ODT} (124 ± 1 °C). The profile was recorded from 85 to 124 °C. The birefringence signal of disordered samples has a magnitude of P/P_0 around 10^{-6}.

To determine the proportionality constant $K(T)$ in eq 9 as a function of temperature for each sample, a fully disordered sample was first quenched to a temperature of interest (for example, 112 °C, quench depth of 12 °C) to monitor the grain structure evolution, and then the sample was further quenched to 90 °C after the first quench was completed. The sample was maintained at 90 °C for at least 8 h, after which we expected the sample to be entirely ordered. A plot of I_0/V as a function of elapsed time for the quench to 90 °C resulted in a curve that asymptotically leveled off to a constant value, which we took to be the value of K at 90 °C (see eq 9). The same sample was then sequentially quenched to 80, 60, 40, and 20 °C, and the sample was held at each of these temperatures for 10 min to ensure that the sample reached thermal equilibrium. Given that $\phi \rightarrow 1$ at the end of the 90 °C quench, one can assume that the sample remains fully ordered during the quenches to lower temperatures. Therefore, the K values at 80, 60, 40 and 20 °C were calculated from $K = I_0/V$ at each temperature. I_0 is represented by a dimensionless number ranging from 0 to 255 that is proportional to the intensity generated by the CCD camera. Therefore, K has units of μm^{-3} in this paper. A least-squares fit of K vs T obtained from 20 to 90 °C revealed a weak linear temperature dependence; see Figure 3. By extrapolation, the K value at temperature 112 °C was estimated to be 0.83 μm^{-3}. The volume fractions of ordered grains over the entire range of temperatures below the T_{ODT} could be determined using eq 9. $K(T)$ was determined separately for each sample studied in this paper. For different samples, there were slight differences between the slopes and intercepts (a and b, respectively in Figure 3) obtained by the least-squares fit. The weak temperature dependence of K is probably the result of the weak temperature dependence of the form birefringence of grains.[14]

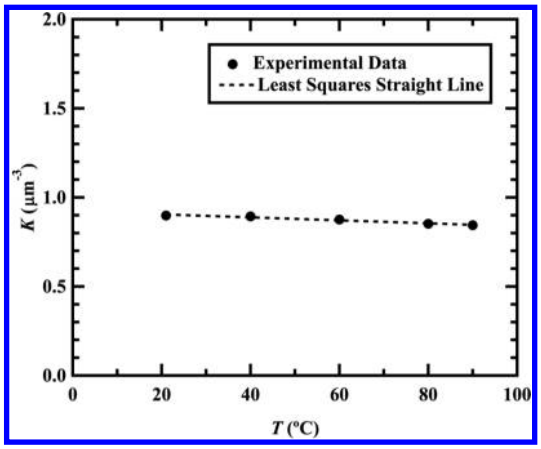

Figure 3. Least squares fitting of proportionality constant K between I_0 and ϕV obtained after grain evolution experiments with a quench depth of 12 °C. The dashed line is described by a linear equation: $y = ax + b$ with a = −0.00083 and b = 0.9204.

The grain density ρ (number of grains per unit volume) is given by[12]

$$\rho = \phi/V \tag{13}$$

RESULTS AND DISCUSSION

Time Dependence of Grain Evolution. Figure 4 shows the DPLS patterns at three different times during the quench with a quench depth of 6 °C (shallow quench). The earliest detectable pattern (an "X" pattern) obtained at t = 28 min is shown in Figure 4a, providing evidence for the fast formation of ellipsoidal grains with a large aspect ratio during the early stages

dx.doi.org/10.1021/ma501166p | Macromolecules 2014, 47, 5784−5792

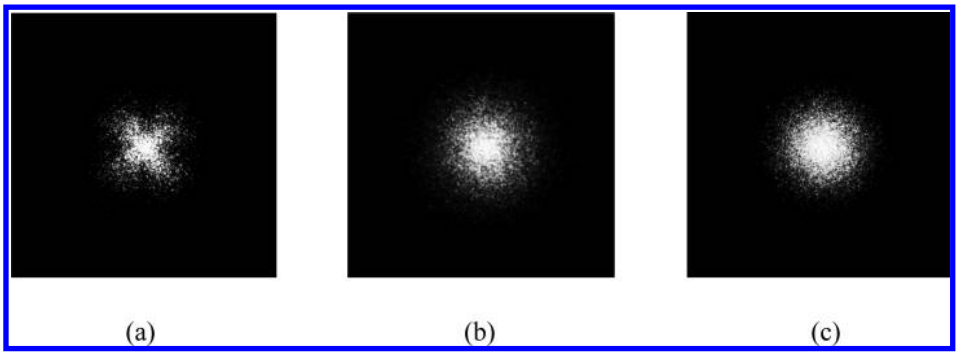

Figure 4. Parts a–c representing depolarized scattering patterns captured at 28, 60 and 400 min, respectively with a sample quenched 6 °C below T_{ODT} (quench depth is 6 °C). The maximum scattering vector q at the sides of each image is 1.13 μm^{-1}. The contrast of each pattern has been adjusted to enhance major features that are not clear in the original low intensity patterns. Polarizer and analyzer are oriented vertically and horizontally in these images.

of the quench. Scattering patterns at later times (Figure 4, parts b and c) exhibit azimuthally symmetric patterns ("O" patterns), indicating the presence of grains with aspect ratios in the vicinity of unity. Figure 5 shows an example of a least-squares

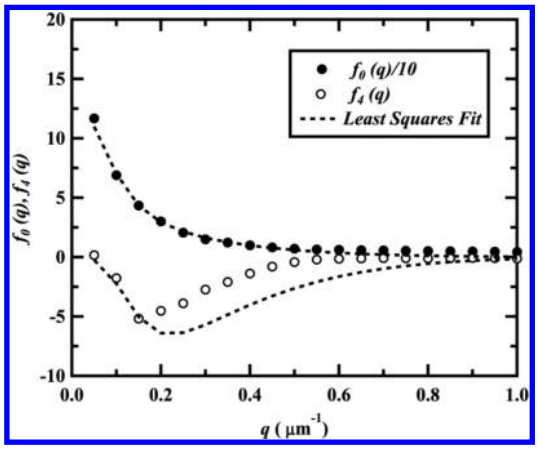

Figure 5. Least squares fit of experimentally extracted $f_0(q)$ and $f_4(q)$ functions from the scattering pattern in Figure 4a. Since the amplitude of $f_0(q)$ was always much larger than $f_4(q)$, both the theoretical curve and experimental data points of $f_0(q)$ are plotted with 1/10 of their actual amplitudes. The grain parameters obtained from this fit are l/w = 7.7, w = 3.5 μm, and I_0 = 21.

fit of $f_0(q)$ and $f_4(q)$ functions extracted from the scattering pattern in Figure 4a using eqs 7 and 8, from which we obtained the grain parameters at 28 min. In this paper, all of the reported values of l, w and I_0 were acquired from such least-squares fits with errors in the range 7–11%. The function f_0 has been divided by 10 in Figure 5 so that both f_0 and f_4 could be conveniently plotted on the same graph. This has the effect of overemphasizing the mismatch between the experimental f_4 points and the least-squares fitted function. We could obtain a better fit of f_4 with a larger value of w and smaller value of l/w, but that would be at the expense of a poorer fit to the tail of f_0. The minimum in f_4 is not captured because the actual block copolymer samples are too complex to be completely captured by the 3-parameter single ellipsoidal grain model. What is remarkable is how well the single ellipsoidal grain model fits the experimental data, in spite of the fact that it greatly simplifies the complexities of actual block copolymer grains (which could, in principle, nucleate and grow at different times and at different rates) using only three parameters. While 4-fold symmetric depolarized light scattering patterns from polymer samples have been studied and interpreted since the 1960s, the reduction of the two-dimensional intensity data to two q-dependent functions, and the simultaneous fitting of these functions to three parameters to quantify scattering size, shape and volume fraction are unique to the approach presented in ref 11 and further developed in this paper. Table 1 summarizes the values of grain parameters (l and w) at early and late times for all three quench depths.

Table 1. Summary of Development of Grain Structures with Quench Depths 6, 12 and 24 °C

quench depth (°C)	elapsed time (min)	pattern	l/w	w (μm)	l (μm)	V (μm^3)	ϕ
6	28	"X"	7.7	3.5	27	330	0.06
6	400	"O"	1.0	7.5	7.5	420	0.33
12	22	"X"	6.5	3.4	22	260	0.09
12	400	nearly "O"	1.2	5.4	6.5	190	0.97
24	9	"X"	6.4	3.6	23	300	0.08
24	400	nearly "O"	1.3	4.4	5.7	110	1.0

Figure 6 shows the time evolution of l/w, l, and w for all three quench temperatures, while Figure 7 shows the time evolution of average grain volume V and grain volume fraction ϕ. The time evolutions of the shallow (quench depth of 6 °C), intermediate (quench depth of 12 °C), and deep (quench depth of 24 °C) quenches share some common features. In all 3 cases, l/w is between six and eight at very early times, but falls to nearly unity at longer times (Figure 6a). The grain length, l, decreases sharply, while grain width, w, increases slightly as the quenches proceed, (Figure 6, parts b and c). In the case of quench depths of 6 and 12 °C, the grain volume peaks at early times (10–30 min) but falls off at longer times (Figure 7, parts a and b).

In the case of the 24 °C quench, the average grain volume decreases with increasing time in the entire experimental window (Figure 7c). The decrease in grain volume with increasing time during isothermal annealing has not been observed in any previous study of block copolymers. It is conceivable that the exchange of salt molecules between the ordered and disordered phases is responsible for this. For quenches into the coexistence region, according to the lever rule, the salt concentration in the disordered phase must be less than the average salt concentration, and the salt concentration

dx.doi.org/10.1021/ma501166p | Macromolecules 2014, 47, 5784–5792

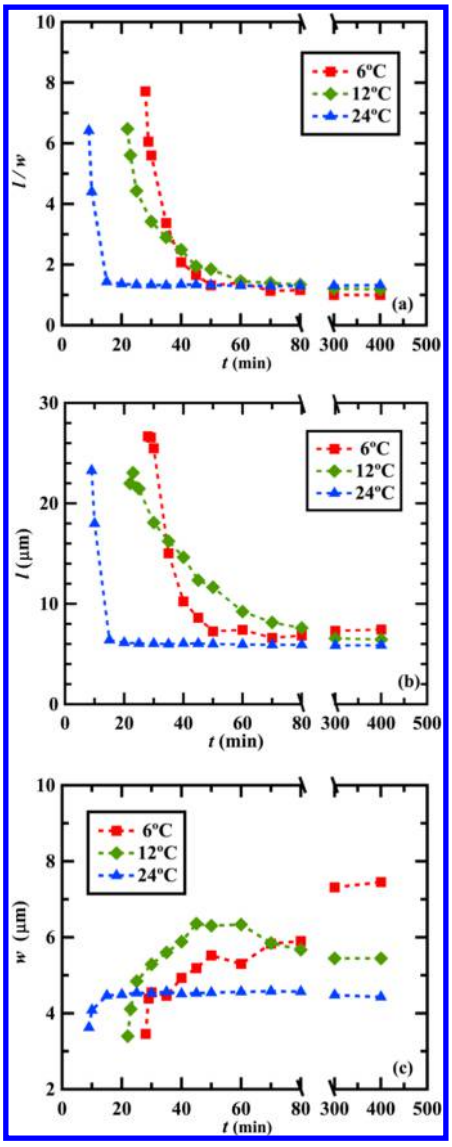

Figure 6. Parts a–c representing the time dependence of length parameters, l/w, l and w, respectively, on the quench depths of 6, 12, and 24 °C.

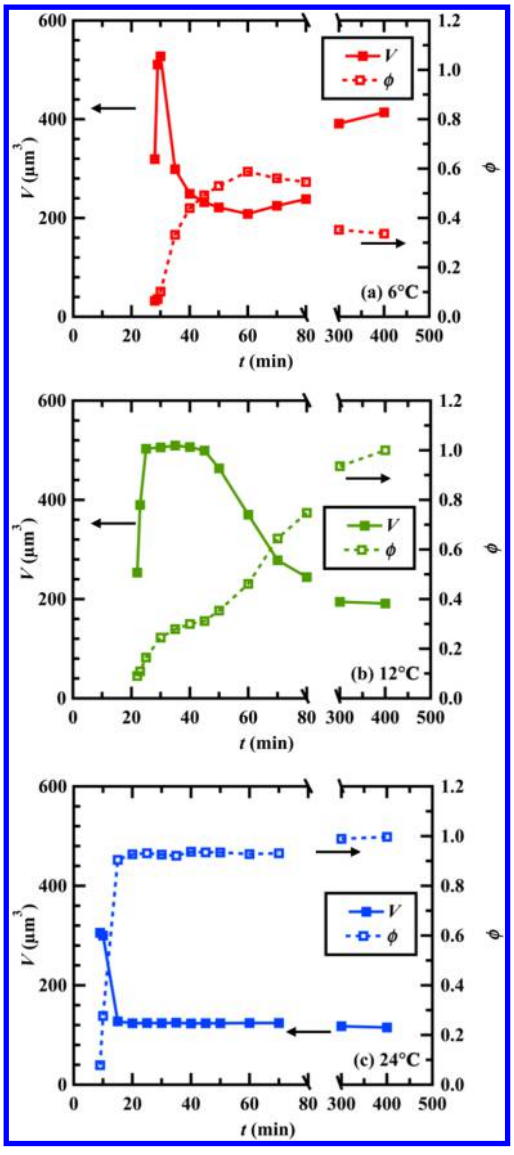

Figure 7. Parts a–c representing the time dependence of the average grain volumes (V) and the volume fractions (ϕ) of ordered phases for quench depths of 6, 12, and 24 °C, respectively.

in the ordered phase must be greater than the average salt concentration—the concentration in the initial disordered phase. Thus, there should be a net diffusion of salt from the disordered phase to the ordered phase until the equilibrium partitioning is reached. However, the driving force for this diffusion only exists after the ordered phase is formed. We hypothesize that grains formed during the early stages, before salt diffusion takes place, are elongated. The subsequent diffusion of salt into the grains results in a more isotropic preferred shape. The preferred shape of grains is governed by the orientation-dependence of the interfacial tension between ordered and disordered phases. While such a calculation for the two systems described above is well outside the scope of the present paper, this kind of calculation has been done for ordered phases formed in pure block copolymers.[5] The mechanism for the transformation from elongated to isotropic grains may be by "pinching off" elongated grains. Alternatively, there may be two types of grains: fast-growing metastable elongated grains containing the same amount of salt as the initial disordered phase, and slower-growing stable isotropic grains that grow at a rate slow enough to allow for salt redistribution and that consume the metastable grains as they grow.

In neat block copolymers, the transition from disorder to order requires concerted rotation of adjacent molecules so that the blocks lie on the same side of the junction. In other words, order formation does not require diffusion of the polymer chains. In our salt-containing system, the polymer volume fraction of samples used in this paper is 0.89, which is estimated by the method described in ref 28, and thus, to a good approximation, order formation does not require the diffusion of polymer chains. However, as the ordered grains are formed, and the order parameter reaches its equilibrium value, there is a driving force for salt to diffuse from the disordered phase into the ordered grains.[36] It is likely that this new phenomenon is responsible for the unexpected decrease in grain volume seen at all quench depths (Figure 7).

At elapsed times greater than 60 min, the average grain volume for the shallow quench (quench depth of 6 °C) increases slowly from 200 to 400 μm^3 over a period of 350 min.

dx.doi.org/10.1021/ma501166p | Macromolecules 2014, 47, 5784–5792

Over the same period, the grain volume fraction decreases from 0.60 to 0.33. In contrast, for intermediate and deep quenches (quench depths of 12 and 24 °C), grain volume decreases monotonically after an early stage of grain growth. Over the same period, the grain volume fraction approaches unity at long times. These observations suggest that the shallow quench lies in the coexistence window, while the others do not.

In Figure 8, we plot grain density as a function of elapsed time for the three quenches. The deep quench is the simplest

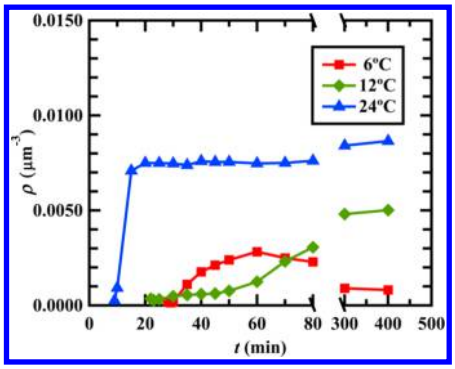

Figure 8. Grain density ρ versus time during the quench at different quench depths.

case; at this temperature, the grain density increases rapidly in about 15 min and grain volume fraction approaches 0.9 at this time. This is followed by a much slower increase in both ρ and ϕ. This suggests that the ordering proceeds by the formation of new grains throughout the duration of the quench. For the intermediate quench, the phenomenology is similar except that the increase in ρ and ϕ are much slower. For the shallow quench depth, ρ decreases at long times ($60 < t < 400$ min) suggesting that at this stage grains may be "melting", i.e., undergoing a transition to disorder.

In the discussion above, we have described three separate experiments performed on three different samples. We have repeated these experiments on many samples and have obtained quantitatively similar data as a function of elapsed time.

Temperature Dependence of Grain Parameters. Figure 9a shows the grain length parameters l and w at 400 min as a function of quench depth, and Figure 9b shows the grain volume and grain volume fraction at 400 min as a function of quench depth. Deeper quenches give rise to higher grain densities and smaller grains, consistent with our earlier studies on neat block copolymers.[11,14] The main new feature is that while the deep quench results in grain volume fractions approaching unity, the shallow quench produces a sample that is 33% ordered and 67% disordered after 400 min. This feature has never been seen in our studies of neat diblock copolymers, but is consistent with the findings of Thelen et al.[37] as well as the theoretical predictions of Nakamura et al.[36] It appears that the shallow quench falls within the coexistence window where we obtain an equilibrium mixture of ordered and disordered phases.

CONCLUSIONS

We have studied structural changes occurring in block copolymer/salt mixtures during quenches from the disordered state to temperatures below the T_{ODT}, where an ordered lamellar phase is formed, using depolarized light scattering. By

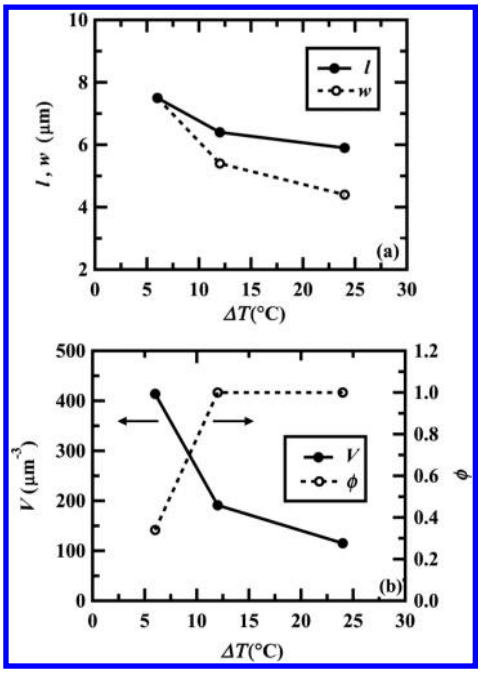

Figure 9. (a) Temperature dependence of the final length parameters l and w of samples with quench depths of 6, 12, and 24 °C at 400 min. (b) Temperature dependence of average grain volumes and volume fractions of ordered phases of samples with quench depths of 6, 12, and 24 °C at 400 min.

analyzing the scattering patterns, we have been able to determine the time dependence of grain size, shape, density and volume fraction. For a shallow quench (quench depth of 6 °C) we see evidence for the coexistence of ordered and disordered regions, which is consistent with the findings of Thelen et al.[37] using SAXS, as well as the theoretical prediction of Nakamura et al.[36] There are, however, some unexpected consequences of adding salt to block copolymers. Highly anisotropic prolate ellipsoidal grains with aspect ratios between six and eight are obtained at early times. In contrast, weakly anisotropic ellipsoids with an aspect ratio of about two are obtained in neat lamellar block copolymers.[5] At all quench depths, the average grain volume first increases and then decreases with increasing time. In neat block copolymers, grain volume increases monotonically with time. Additional work is needed to uncover the microscopic underpinnings nucleation, growth, and eventual contraction of ordered grains in block copolymer/salt mixtures.

AUTHOR INFORMATION

Corresponding Author

*(B.A.G.) E-mail: bgaretz@nyu.edu.

Present Address

¶(I.N.) State Key Laboratory of Polymer Physics and Chemistry, Changchun Institute of Applied Chemistry, Chinese Academy of Sciences, Changchun, 130022, P. R. China

Notes

The authors declare no competing financial interest.

ACKNOWLEDGMENTS

The authors acknowledge the generous support of the National Science Foundation through Award Numbers DMR-0966626, DMR-0966765, and CBET-0965812. Any opinions, findings, and conclusions or recommendations expressed in this paper

are those of the authors and do not necessarily reflect the views of the National Science Foundation. The assistance of Mr. Hao-Chun Chiang in solving some programming problems is also appreciated

■ ABBREVIATIONS

CCD	charge coupled device
DPLS	depolarized light scattering
TIFF	tagged image file format
LiTFSI	lithium bis(trifluoromethanesulfonyl)imide
OCT	order−coexistence transition
ODT	order−disorder transition
PDI	polydispersity index
PEO	poly(ethylene oxide)
PS	polystyrene
SAXS	small angle X-ray scattering
SEO	polystyrene-*b*-poly(ethylene oxide) diblock copolymer

Symbols

d	distance between the sample and screen, mm
$C_0(q;l,w)$	azimuthally symmetric component of theoretical scattered intensity, dimensionless
$C_4(q;l,w)$	4-fold modulated component of theoretical scattered intensity, dimensionless
$f_0(q)$	zeroth cosine moment of experimental scattered intensity, dimensionless
$f_4(q)$	fourth cosine moment of experimental scattered intensity, dimensionless
$I(q,\mu)$	experimental scattered intensity as a function of q and μ, dimensionless
I_0	experimental scattered intensity in forward direction, $q = 0$, dimensionless
K, $K(T)$	proportionality constant, as a function of temperature, μm^{-3}
L_S	thickness of SEO/LiTFSI sample, mm
l	average grain length, μm
M_{PEO}	number-average molecular weight of PEO block, kg mol^{-1}
M_{PS}	number-average molecular weight of PS block, kg mol^{-1}
n	average refractive index of SEO/LiTFSI samples, dimensionless
Δn	difference between extraordinary and ordinary refractive index of grains, n_e and n_o, respectively, dimensionless
q	magnitude of scattering vector, μm^{-1}
P	total depolarized transmitted power, mW
P_0	incident laser power, mW
r	lithium salt concentration, dimensionless
T_{OCT}	order-to-coexistence transition temperature
T_{ODT}	order-to-disorder transition temperature
V	average grain volume, μm^3
w	average grain width, μm
(x, y)	Cartesian coordinates of location on the scattering pattern

Greek Letters

χ	Flory−Huggins interaction parameter, dimensionless
ϕ	grain volume fraction, dimensionless
λ	wavelength of incident light, nm
θ	polar scattering angle, rad
μ	azimuthal scattering angle, rad
ρ	average grain density, number of grains per unit volume, μm^{-3}

■ REFERENCES

(1) Quartarone, E.; Mustarelli, P. Electrolytes for solid-state lithium rechargeable batteries: recent advances and perspectives. *Chem. Soc. Rev.* **2011**, *40* (5), 2525−2540.
(2) Young, W. S.; Kuan, W. F.; Epps, T. H. Block Copolymer Electrolytes for Rechargeable Lithium Batteries. *J. Polym. Sci., Polym. Phys.* **2014**, *52* (1), 1−16.
(3) Hallinan, D. T.; Balsara, N. P. Polymer Electrolytes. *Annu. Rev. Mater. Res.* **2013**, *43*, 503−525.
(4) Stone, G. M.; Mullin, S. A.; Teran, A. A.; Hallinan, D. T.; Minor, A. M.; Hexemer, A.; Balsara, N. P. Resolution of the Modulus versus Adhesion Dilemma in Solid Polymer Electrolytes for Rechargeable Lithium Metal Batteries. *J. Electrochem. Soc.* **2012**, *159* (3), A222−A227.
(5) Balsara, N. P.; Marques, C. M.; Garetz, B. A.; Newstein, M. C.; Gido, S. P. Anisotropy of lamellar block copolymer grains. *Phys. Rev. E* **2002**, *66* (5), 052802.
(6) Lin, C. C.; Jonnalagadda, S. V.; Kesani, P. K.; Dai, H. J.; Balsara, N. P. Effect of Molecular-Structure on the Thermodynamics of Block-Copolymer Melts. *Macromolecules* **1994**, *27* (26), 7769−7780.
(7) Fredrickson, G. H.; Helfand, E. Fluctuation Effects in the Theory of Microphase Separation in Block Copolymers. *J. Chem. Phys.* **1987**, *87* (1), 697−705.
(8) Bates, F. S. Polymer-Polymer Phase-Behavior. *Science* **1991**, *251* (4996), 898−905.
(9) Leibler, L. Theory of Microphase Separation in Block Co-Polymers. *Macromolecules* **1980**, *13* (6), 1602−1617.
(10) Dai, H. J.; Balsara, N. P.; Garetz, B. A.; Newstein, M. C. Grain growth and defect annihilation in block copolymers. *Phys. Rev. Lett.* **1996**, *77* (17), 3677−3680.
(11) Newstein, M. C.; Garetz, B. A.; Balsara, N. P.; Chang, M. Y.; Dai, H. J. Growth of grains and correlated grain clusters in a block copolymer melt. *Macromolecules* **1998**, *31* (1), 64−76.
(12) Kim, W. G.; Garetz, B. A.; Newstein, M. C.; Balsara, N. P. Maximizing the grain growth rate during the disorder-to-order transition in block copolymer melts. *J. Polym. Sci., Polym. Phys.* **2001**, *39* (19), 2231−2242.
(13) Lin, C. C.; Jeon, H. S.; Balsara, N. P.; Hammouda, B. Spinodal Decomposition in Multicomponent Polymer Blends. *J. Chem. Phys.* **1995**, *103* (5), 1957−1971.
(14) Kim, W. G.; Chang, M. Y.; Garetz, B. A.; Newstein, M. C.; Balsara, N. P.; Lee, J. H.; Hahn, H.; Patel, S. S. Effect of quench depth on grain structure in quiescently ordered block copolymers. *J. Chem. Phys.* **2001**, *114* (22), 10196−10211.
(15) Lo, T. Y.; Ho, R. M.; Georgopanos, P.; Avgeropoulos, A.; Hashimoto, T. Direct Visualization of Order-Order Transitions in Silicon-Containing Block Copolymers by Electron Tomography. *ACS Macro Lett.* **2013**, *2* (3), 190−194.
(16) Chastek, T. Q.; Lodge, T. P. Grain shapes and growth kinetics during self-assembly of block copolymers. *J. Polym. Sci., Polym. Phys.* **2006**, *44* (3), 481−491.
(17) Campbell, I. P.; Lau, G. J.; Feaver, J. L.; Stoykovich, M. P. Network Connectivity and Long-Range Continuity of Lamellar Morphologies in Block Copolymer Thin Films. *Macromolecules* **2012**, *45* (3), 1587−1594.
(18) Hashimoto, T.; Sakamoto, N.; Koga, T. Nucleation and growth of anisotropic grain in block copolymers near order-disorder transition. *Phys. Rev. E* **1996**, *54* (5), 5832−5835.
(19) Ryu, H. J.; Fortner, D. B.; Lee, S.; Ferebee, R.; De Graef, M.; Misichronis, K.; Avgeropoulos, A.; Bockstaller, M. R. Role of Grain Boundary Defects During Grain Coarsening of Lamellar Block Copolymers. *Macromolecules* **2013**, *46* (1), 204−215.
(20) Ryu, H. J.; Sun, J.; Avgeropoulos, A.; Bockstaller, M. R. Retardation of Grain Growth and Grain Boundary Pinning in Athermal Block Copolymer Blend Systems. *Macromolecules* **2014**, *47* (4), 1419−1427.
(21) Kang, H.; Detcheverry, F. A.; Mangham, A. N.; Stoykovich, M. P.; Daoulas, K. C.; Hamers, R. J.; Muller, M.; de Pablo, J. J.; Nealey, P. F. Hierarchical assembly of nanoparticle superstructures from block

copolymer-nanoparticle composites. *Phys. Rev. Lett.* **2008**, *100* (14), 148303.
(22) Olsen, B. D.; Li, X. F.; Wang, J.; Segalman, R. A. Near-surface and internal lamellar structure and orientation in thin films of rod-coil block copolymers. *Soft Matter* **2009**, *5* (1), 182−192.
(23) Gido, S. P.; Gunther, J.; Thomas, E. L.; Hoffman, D. Lamellar Diblock Copolymer Grain-Boundary Morphology 0.1. Twist Boundary Characterization. *Macromolecules* **1993**, *26* (17), 4506−4520.
(24) Hosoda, T.; Gido, S. P.; Mays, J. W.; Huang, T. Z.; Park, C. R.; Yamada, T. Effect of solvents and thermal annealing on the morphology development of a novel block copolymer ionomer: a case study of sulfonated polystyrene-block-fluorinated polyisoprene. *J. Polym. Eng.* **2013**, *33* (2), 191−191.
(25) Hou, J. B.; Li, J.; Madsen, L. A. Anisotropy and Transport in Poly(arylene ether sulfone) Hydrophilic-Hydrophobic Block Copolymers. *Macromolecules* **2010**, *43* (1), 347−353.
(26) Nakamura, I.; Wang, Z. G. Salt-doped block copolymers: ion distribution, domain spacing and effective chi parameter. *Soft Matter* **2012**, *8* (36), 9356−9367.
(27) Gunkel, I.; Thurn-Albrecht, T. Thermodynamic and Structural Changes in Ion-Containing Symmetric Diblock Copolymers: A Small-Angle X-ray Scattering Study. *Macromolecules* **2012**, *45* (1), 283−291.
(28) Teran, A. A.; Balsara, N. P. Thermodynamics of Block Copolymers with and without Salt. *J. Phys. Chem. B* **2014**, *118* (1), 4−17.
(29) Nakamura, I.; Balsara, N. P.; Wang, Z. G. Thermodynamics of Ion-Containing Polymer Blends and Block Copolymers. *Phys. Rev. Lett.* **2011**, *107* (19), 5.
(30) Huang, J.; Tong, Z. Z.; Zhou, B.; Xu, J. T.; Fan, Z. Q. Salt-induced microphase separation in poly(epsilon-caprolactone)-b-poly-(ethylene oxide) block copolymer. *Polymer* **2013**, *54* (12), 3098−3106.
(31) Mori, K.; Okawara, A.; Hashimoto, T. Order-disorder transition of polystyrene-block-polyisoprene 1. Thermal concentration fluctuations in single-phase melts and solutions and determination of chi as a function of molecular weight and composition. *J. Chem. Phys.* **1996**, *104* (19), 7765−7777.
(32) Young, W. S.; Epps, T. H. Salt Doping in PEO-Containing Block Copolymers: Counterion and Concentration Effects. *Macromolecules* **2009**, *42* (7), 2672−2678.
(33) Young, W. S.; Albert, J. N. L.; Schantz, A. B.; Epps, T. H. Mixed-Salt Effects on the Ionic Conductivity of Lithium-Doped PEO-Containing Block Copolymers. *Macromolecules* **2011**, *44* (20), 8116−8123.
(34) Naidu, S.; Ahn, H.; Gong, J.; Kim, B.; Ryu, D. Y. Phase Behavior and Ionic Conductivity of Lithium Perchlorate-Doped Polystyrene-b-poly(2-vinylpyridine) Copolymer. *Macromolecules* **2011**, *44* (15), 6085−6093.
(35) Wu, K. A.; Jha, P. K.; de la Cruz, M. O. Control of Nanophases in Polyelectrolyte Gels by Salt Addition. *Macromolecules* **2010**, *43* (21), 9160−9167.
(36) Nakamura, I.; Balsara, N. P.; Wang, Z. G. First-Order Disordered-to-Lamellar Phase Transition in Lithium Salt-Doped Block Copolymers. *ACS Macro Lett.* **2013**, *2* (6), 478−481.
(37) Thelen, J. L.; Teran, A. A.; Wang, X.; Garetz, B. A.; Nakamura, I.; Wang, Z. G.; Balsara, N. P. Phase Behavior of a Block Copolymer/Salt Mixture through the Order-to-Disorder Transition. *Macromolecules* **2014**, *47* (8), 2666−2673.
(38) Newstein, M. C.; Garetz, B. A.; Dai, H. J.; Balsara, N. P. Light-Scattering and Microscopy from Block-Copolymers with Cylindrical Morphology. *Macromolecules* **1995**, *28* (13), 4587−4597.
(39) Balsara, N. P.; Perahia, D.; Safinya, C. R.; Tirrell, M.; Lodge, T. P. Birefringence Detection of the Order-to-Disorder Transition in Block Copolymer Liquids. *Macromolecules* **1992**, *25* (15), 3896−3901.
(40) Garetz, B. A.; Balsara, N. P.; Dai, H. J.; Wang, Z.; Newstein, M. C.; Majumdar, B. Orientation correlations in lamellar block copolymers. *Macromolecules* **1996**, *29* (13), 4675−4679.